JPRS-JST-91-009
25 FEBRUARY 1991

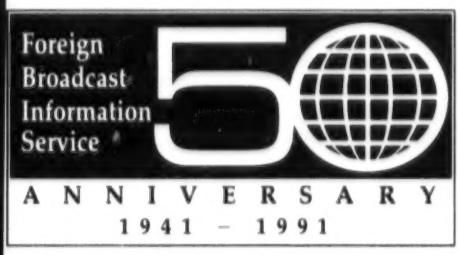

JPRS Report

Science & Technology

Japan

STRUCTURAL TRANSITION OF SERUM ALBUMIN

JPRS-JST-91-009
25 FEBRUARY 1991

SCIENCE & TECHNOLOGY

JAPAN

STRUCTURAL TRANSITION OF SERUM ALBUMIN

91FE0003 Tokyo KEISHA KINO ZAIRYO KENKYUKAI in Japanese 22 May 90 pp 7-17

[Article by M. Sogami and S. Era, Second Physiology Department, School of Medicine, Gifu University; selections from proceedings of the Ninth Functionally Gradient Materials Workshop held on 22 May 90]

CONTENTS

Structural Transition of Serum Albumin

91FE0003 Tokyo KEISHA KINO ZAIRYO KENKYUKAI in Japanese 22 May 90 pp 7-17

[Article by M. Sogami and S. Era, Second Physiology Department, School of Medicine, Gifu University; selections from proceedings of the Ninth Functionally Gradient Materials Workshop held on 22 May 90]

[Text] Introduction

Unlike the two previous topics, the content of this lecture deals extensively with the physical chemistry of the subject. I will discuss clinical applications at the end.

Fig. 1 shows the linear structural model of human serum albumin of Brown[1-3]. Unlike the diagram shown by the previous lecturer, subdomain 1AB (1AX, 1AY, 1ABZ) and subdomain 1C (1CX, 1CY, 1CZ) of domain 1 are opposed to each other. The subdomains are mutually opposed in domain 2 and domain 3 as well.

I shall briefly explain the properties of serum albumin by using domain 1 as an example. First, I shall explain why subdomains 1AB and 1C are opposed to each other. Domain 1 has a helical segment in the area marked with big arrows, and the α-helix dipoles are facing the direction of the arrows (toward N-terminal). Subdomain 1C is shown turned around so that the domain is electrostatically stable[1,3]. And, regions 102-123, 290-315, and 488-513 are equivalent to Brown's hinge. Fig. 1 shows from the top subdomains 1AB, 1C, 2AB, 2C, 3AB, and 3C. The distance between Trp-214 and Tyr-411 is approximately 18 Å at neutral pH and 24 Å at pH 9[4]. This distance expands to approximately 30 Å in the acidic side. There is one SH group at Cys-34 and as shown in Fig. 1, 17 S-S bonds.

The three domains of serum albumin having the structure described above are arranged as shown in Fig. 1 like meatballs skewered on a stick; domain 1, domain 2, and domain 3 (Brown, 1982). Recently, Brown (1988) modified this model slightly and presented a report[5] at the International Biochemistry meeting stating that domain 1 and domain 3 may not be as far apart as they appear on the skewered meatball model, but are closer together. The amounts of α-helix and ß-structure of plasma (serum) albumin having such a structure are 70% and 15% respectively[6,7] (See footnote at the end of the text).

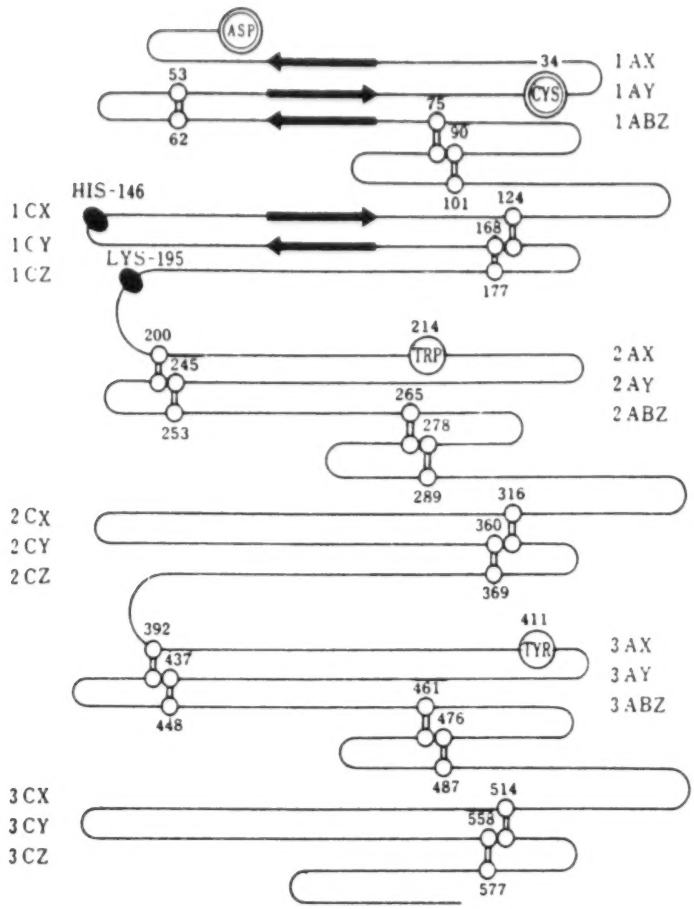

Fig. 1 Model diagram of human serum albumin molecule[3]. Cys-34: SH group; o=o: S-S bond; His-146 (•) and Lys-195 (•): a part[42] of the binding site of an indole compound. Domain 1 (subdomain 1AB (1AX, 1AY, 1ABZ) and subdomain 1C (1CX, 1CY, 1CZ)), domain 2 (subdomain 2AB (2AX, 2AY, 2ABZ) and subdomain 2C (2CX, 2CY, 2CZ)), and subdomain 2C (2CX, 2CY, 2CZ)), domain 3 (subdomain 3AB (3AX, 3AY, 3ABZ) and subdomain 3C (3CX, 3CY, 3CZ)[1,2]. ←:shows the direction of the dipoles in the helical segments.

Plasma (serum) albumin having three domains undergoes highly diverse structural transitions as shown in Table 1. On the acidic side, an N→F transition occurs at pH 4.5-3.8; at still lower pH, F→E transition, or a structural transition called acid expansion[3,8] occurs. At pH 7.0-9.0, an N→B transition[3,8] occurs, and in the same pH region, the SH group of Cys-34 acts as a catalyst and recombines the intramolecular S-S bonds (SH/S-S exchange reaction, *N-A* isomerization reaction). This reaction is also called molecular aging[3,8-15]. In addition, the SH group of Cys-34 acts as an oxidation-reduction buffer system in the bloodstream by binding with and separating from sulfur-containing amino acids in the body undergoing mercapt-nonmercapt conversions (reduction-oxidation reaction)[16-19].

Table 1 表 1

1. $N + nH^+ \rightleftarrows F$ (pH 3.75～4.50)
2. $N \rightleftarrows B + qH^+$ (pH 7.0～9.0)
3. $N \rightleftarrows A + rH^+$
SH, S-S
Exchange
Reaction
4. Mercapt-nonmercapt Conversion

I. N→F transition and F→E transition

In some of the structural transition experiments on acidic side, i.e., N→F transition and F→E transition we are about to explain, specially purified plasma (serum) albumin was used. Among plasma (serum) albumins, some has about 70% SH groups. In the case of cows, it is called bovine mercaptalbumin; BMA). BMA subfractions are further isolated for use in the experiments[7,14,15,20]. The difference is that, in case of crystalline bovine plasma albumin (BPA), the Hill coefficient of the solubility pH dependency (pH solubility profile) in 3.0M KCl is 4~5, whereas the Hill coefficient of BMA which is fractionated and purified as above, is 17~18[3,20]. In the diagrams I am about to show, where the experiments are marked BMA, we used subfractions of BMA with very high purity.

Molecular volumes increase in the N→F transition and F→E transition (acid expansion). The intrinsic viscosity which will become the index for molecular volume for N-, F-, and E-type are 3.7, 4.4, and 8.3 ml/g, respectively[2]. The intrinsic viscosity is proportional to the product of the volume per 1 g protein ($\bar{v}(ml/g)$ and a function of the molecular shape (ν). The N→F transition is suggestive of a slight increase in molecular volume. Fig. 2 shows how the secondary structure (α-helix (○) and ß-structure (•)) of BMA is altered in the N→F and F→E transitions. The α-helix content decreases approximately 10% in the N→F transition, and further decreases another 10% or so in the F→E transition. In other words, the secondary structure of BMA undergoes a two-step alteration on the acidic region corresponding to N→F and F→E transitions.

There is a method called solvent perturbation difference spectroscopy for studying global structural alterations in N→F and F→E transitions[22]. For example, the Stokes diameter of sucrose is 9.4 Å, and that of ethylene glycol is 4.4 Å. Solvent perturbation difference spectroscopy measures the difference spectra of BPA in solvents with and without 20% of the above compounds. Using this method, one can determine in which of the N→F or F→E transitions the crevices open where Tyr and Trp are present in the protein molecules. For sucrose, the crevices open in two steps during the N→F transition and the F→E transition (acid expansion). In other words, crevices of approximately 10 Å in width were formed in the N→F and F→E transitions. However, in the case of a solvent containing 20% ethylene glycol, no change occurs in the structural transitions. Crevices, where Tyr and Trp are located near the surface of the molecule, are open at least ~4 Å, and the crevices seem to open at least to a width of more than 10 Å during the N→F and F→E transitions. Kaplan, et al. labelled the SH group of Cys-34 of BPA with a nitroxide spin probe and, using

ESR [electron spin resonance], discovered that the relaxation time of rotation of the spin probe is shortened during the N→F transition and the F→E transition (acid expansion)[23-25]. In other words, Kaplan, et al. inferred that the SH group of Cys-34 is located at the bottom of the crevice about 10 Å deep in the molecule, and the crevices in the vicinity of the SH group open in two steps during N→F and F→E transitions[23-25]. Fig. 3 shows the relationship of BPA's ability to bind pentane (right) or butane (left) and the N→F transition[26]. BPA's ability to bind hydrophobic butane and pentane disappears in the pH region where the molecular crevices open, i.e., in the N→F transition. In addition, bonds between indole compounds such as Trp and BPA also disappear in exactly the same pH region as above[27].

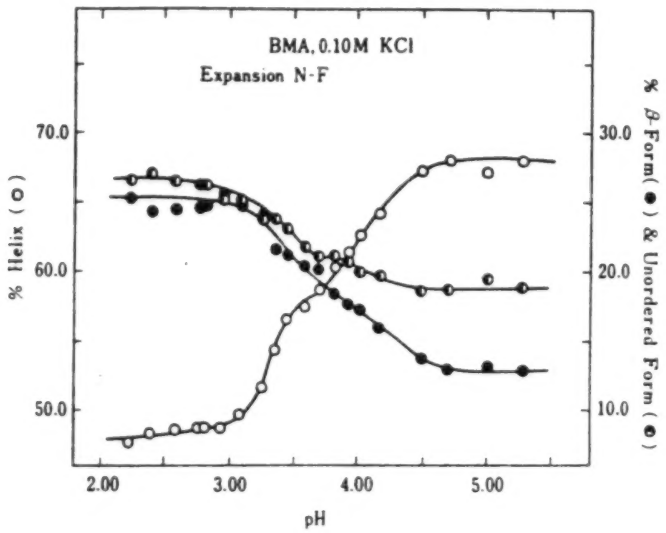

Fig. 2 Secondary structural alterations of bovine mercaptalbumin (BMA) in N→F transition (N-F) and F→E transition (expansion) (0.10 M KCl). ○: α-helix; •: ß structure; ◐: random coil.

Thus far, I have presented experimental results related to intramolecular crevices. I shall now explain experimental results related to molecular rigidity. In this method, a specific site of a protein molecule is irradiated (f_2 irradiation) with radiowaves using an ^{1}H-NMR and the rigidity of the molecule is studied by measuring the spin diffusion speed. We shall consider an S-spin system and an I-spin system as shown in Fig. 4. When the S-spin system is f_2-irradiated using radiowaves, S-spin system magnetization immediately drops to zero as shown by the top curve in Fig. 4. Thereafter, spin diffusion to the I-spin system occurs resulting in decreased magnetization of the I-spin system as well. T_1* shown in Fig. 4 is obtained from this descending curve. $1/T_1^*=1/T_1+1/T_{IS}$ where T_1 and T_{IS} are the vertical relaxation time and cross-relaxation time, respectively. When the rigidity of the protein molecule decreases, the T_{IS} value is elongated[7,28,29]. f_2(ppm) in Table 2 corresponds to an f_2-irradiation site; e.g., 8.65, 7.13, 4.72, 0.40 ppm, corresponding respectively to the C2H of His, aromatic proton, $C_\alpha H$, and $-CH_3$. $\gamma H_2/2\pi$ indicates the strength of f_2-irradiation. The T_{IS} values for $-CH_3$ which were obtained by f_2-irradiation of 8.65 ppm with $\gamma H_2/2\pi$~107 Hz are approximately 0.7

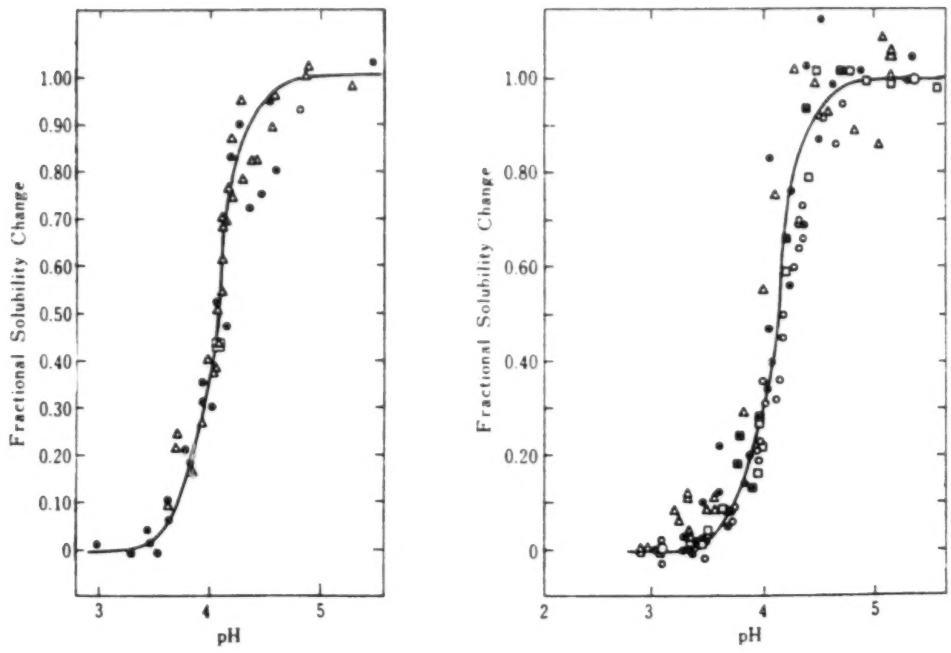

Fig. 3 Changes in the ability of bovine plasma albumin to bind butane (left) and pentane (right) during N→F transition (0.15M NaCl, 25°C)[26]

sec for the N form, approximately 1 sec for the F form, and approximately 1.8 sec for the E form (Table 2)[30]. A similar trend exists when 7.13, 4.72, 0.40, and -2.45 ppm were f_2-irradiated. As explained above, the rigidity of the molecules decreases as the structural transition progresses from N-form → F-form → E-form.

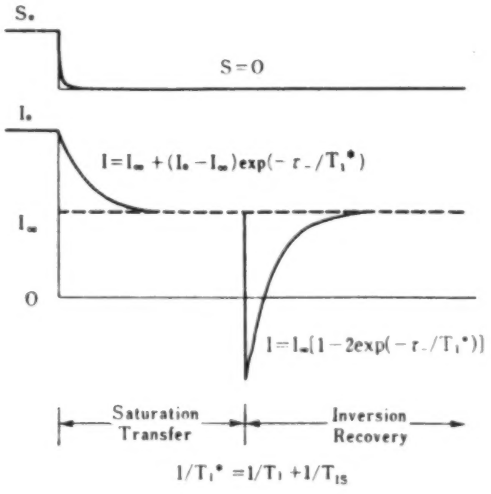

Fig. 4 Model diagram for a technique to determine cross-relaxation phenomenon and cross-relaxation time (T_{1S})[28,29]. See text for explanation.

Table 2

表 2 Cross-Relaxation Times Obtained by the Inversion Recovery Method in Acidic Region

pD(form)	f_2(ppm)	$\gamma H_2/2\pi$(Hz)	T_{1S}(sec) $-CH_3$	$\varepsilon-CH_2$	Arom
5.31 (N)	8.65	107	0.67	0.53	0.78
4.00 (F)	8.65	107	1.01	0.87	0.74
2.96 (E)	8.65	107	1.75	1.59	3.45
5.31 (N)	7.13	69	0.61	0.65	
4.00 (F)	7.13	69	1.32	1.37	
2.96 (E)	7.13	69	1.54	1.43	
5.31 (N)	4.72	20	1.16	1.32	1.45
4.00 (F)	4.72	20	1.37	1.39	1.37
2.96 (E)	4.72	20	2.04	2.08	1.70
5.31 (N)	0.40	39	0.74	0.44	0.81
4.00 (F)	0.40	39	0.82	0.80	1.01
2.96 (E)	0.40	39	1.21	1.52	1.35
5.31 (N)	−2.45	107	0.73	0.73	0.89
4.00 (F)	−2.45	107	1.24	1.21	1.03

N→F Transition (pD 4.8→4.2, 0.10 M Cl^-)
F→E Transition (pD 4.0→3.2, 0.10 M Cl^-)

These changes occurred not only during T_{IS} (cross-relaxation time), but the same changes were observed in the spin echo spectrum using a pulse system to measure the horizontal relaxation time. The spin echo ^{1}H-NMR spectrum is shown in Fig. 5, the bottom graph is for the N-form, the middle one is for the F-form, and the top one is for the E-form[30]. The higher the peaks in Fig. 5, the more mobile the side chains of the protein. In other words, they are not very mobile in the N-form but are highly mobile in the F-form. The same results were obtained in measurements with other than ^{1}H-NMR. Regarding the increased mobility of the charged side chain in the N→F transition, it has been reported that, the analysis of acid titration data with corrected BPA surface potential showed that, in the N-form, 50% of $-COO^-$, form ionic bond with side chains having positive charges; while in F-form, these inter-side chain ionic bonds disappear, and the charged side chains become mobile.[7,31].

In summary, during the N→F transition, the molecular volume increases slightly[21], the α-helix content decreases in the N→F transition[6,7], the crevices on the molecular surface open[22,24,25], ability to bind butane, pentane, etc. disappears[26], the molecules become more flexible[7], and the side chains become mobile as demonstrated by the spin-echo ^{1}H-NMR spectrum[30]. This is a global explanation of the N→F transition at the acidic side of the albumin molecule.

II. N→B transition[3,8]

As shown in Table 1, the N→B transition is a structural transition of plasma (serum) albumin at pH 7.0→9.0. Fig. 6 shows the pH dependence of the angle of rotation at 300nm, $-[\alpha]_{300}$ published by the Purdue University group in 1974[32-34]. In 0.10~0.16 M KCl or in NaCl, $-[\alpha]_{300}$ decreases between pH 7→9. However, exactly as in blood, if 0.002 M Ca^{2+} is present, the pH region of the $-[\alpha]_{300}$ change moves far to the acidic side, and the midpoint pH of $-[\alpha]_{300}$ becomes

about pH 7.5. The $-[\alpha]_{300}$~ $-[\alpha]_{313}$ mainly reflects tertiary structural changes[35,36]. When 0.002 M Ca^{2+} is present, a tertiary structural change with a midpoint at the same site as in body pH is observed. The Hill coefficient obtained from the pH dependence of $-[\alpha]_{300}$ is 1.0 without Ca^{2+} and 2.7 in the presence of 0.002 M Ca^{2+}. In other words, in the presence of Ca^{2+}, the structural transition becomes very cooperative[34].

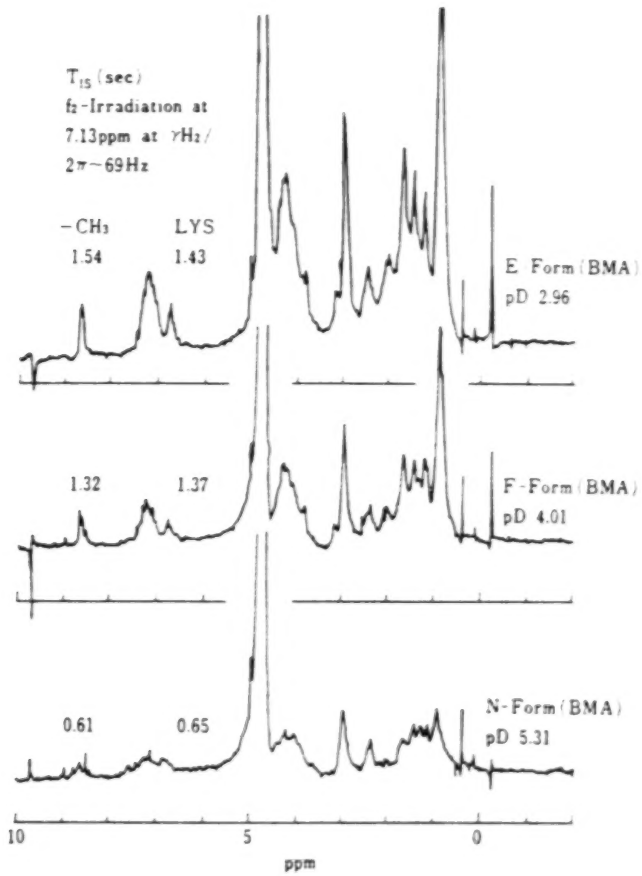

Fig. 5 Spin-echo spectra (0.02 sec CPMG spectra) of bovine mercaptalbumin (BMA) in N-, F-, and E-forms measured with $[90°-(\tau-180°-\tau)_n]$ spin-echo pulse system (τ=0.001 sec, n=10). Shown on the left side is the cross-relaxation time (T_{1S})[32] for f_2-irradiation of 7.13 ppm (aromatic proton) at $\gamma H_2/2\pi$~69 Hz. 4.80%, 0.10 M Cl^-.

Fig. 6 $[\alpha]_{300}$-pH profile of bovine plasma albumin in which the SH group is chemically modified with iodo-acetamide[34]. •:0.16 M NaCl; ○:0.154 M NaCl-0.002 M $CaCl_2$. (Zurawski & Foster, 1974)

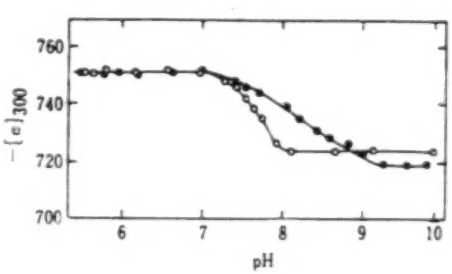

Next, when the pH dependence of 260-310 nm molecular ellipticity ([θ]), which reflects microenvironment such as side chains, is measured, information regarding tertiary structural changes can be obtained. The pH dependence of $-[\theta]_{262}$, $-[\theta]_{268}$, etc. in 0.194 M KCl and 0.002 M $CaCl_2$ is shown in Fig. 7. As seen in Fig. 7, a two-step change is observed, the area shown with arrows (→) correspond to $-[\alpha]_{300}$ changes shown in Fig. 6. Subsequently, slight changes in $-[\theta]_{262}$ and $-[\theta]_{268}$ occur as shown in Fig. 7. The $-[\theta]_{262}$ and $-[\theta]_{268}$ are molecular ellipticities that reflect changes in the vicinity of the S-S bonds[37,38]. This two-step change at pH 7~9 is not observed in 0.20 M KCl (Fig. 7, ---, midpoint→).

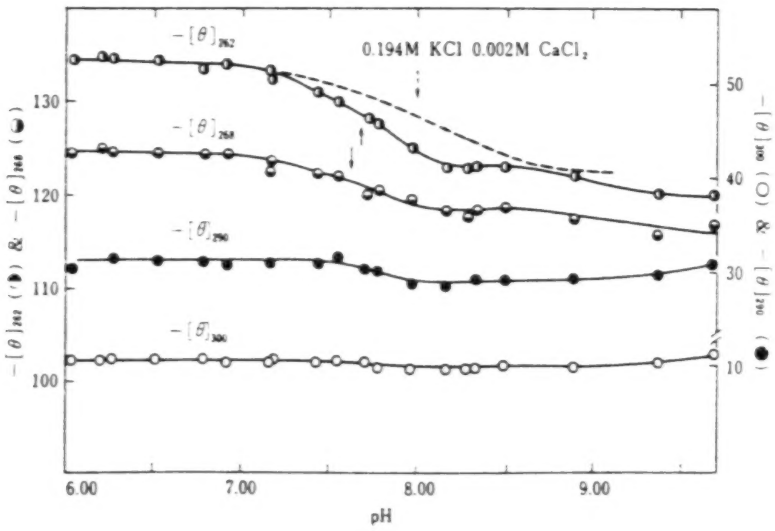

Fig. 7 $[\theta]_{262}$, $[\theta]_{268}$, $[\theta]_{290}$, and $[\theta]_{300}$ pH profiles of bovine plasma albumin (0.194 M KCl-0.002 M $CaCl_2$)[37]. ·····: $[\theta]_{262}$-pH profile in 0.200 M KCl.

Zurawski, et al. labelled the SH groups of Cys-34 with a ^{19}F compound and studied the N→B transition by means of the chemical shifting of ^{19}F-NMR and observed the two-step change shown in Fig. 7 when Ca^{2+} was present[34]. Kaplan, et al. labelled the SH groups of Cys-34 with a nitroxide spin probe, determined the changes in the N→B transition during the spin probe rotary relaxation time, and reported[25] that the rotary relaxation time decreases in two steps the same as $-[\theta]_{262}$ and $-[\theta]_{268}$ of Fig. 7. The above-mentioned report suggests that the tertiary structure in the N→B transition undergoes a two-step alteration. This inference is not contradictory to the results shown in Fig. 6 due to the following reason. The group of Van Os, et al. reported[39] that $-[\alpha]_{300-313}$ mainly reflects only the tertiary structural changes of the N-terminal fragments of BPA.

We shall explain secondary structural alterations in the N→B structure. In these experiments, the refined, super special grade BMA as described in the paragraphs related to the N→F transition is not used, but simply crystalline BPA is used. The number of α-helices in 0.10 M KCl gradually decreases in the pH 7~9 range, and ß-structures gradually increase in number. Compared to tertiary structural changes, secondary structural alterations are not as drastic.

Although the secondary structural changes in Fig. 8 are slight, a comparison with Fig. 9 (~0 ionic strength) reveals that it is not an error. In addition, in order to prevent the *N-A* isomerization reaction (intramolecular SH/S-S exchange reaction) explained in Table 1, BPA in which the SH groups of Cys-34 were chemically modified with iodoacetamide (IA-BPA) was used in the experiments summarized in Figs. 8 and 9[3,37]. In a salt-free state other than alkali for pH adjustment, i.e., at an ~0 ionic strength (Fig. 9, no added salt), a clear secondary structural alteration is observed in the pH region of the N→B transition of IA-BPA shown in Fig. 9. The α-helix content decreased approximately 8% at pH 7~9 in the N→B transition, and ß-structures increase as shown in the diagram. If the SH groups of Cys-34 are not chemically modified, the intramolecular SH/S-S exchange reaction explained below occurs in the pH 7~9 region at an ~0 ionic strength (no added salt). When KCl is added at pH 8.6~8.7 as shown in Fig. 9 (mostly B-form structure), the α-helix content increases cooperatively between 0.025~0.05 M, but it does not increase even though the concentration is increased above 0.05 M (Fig. 16)[37].

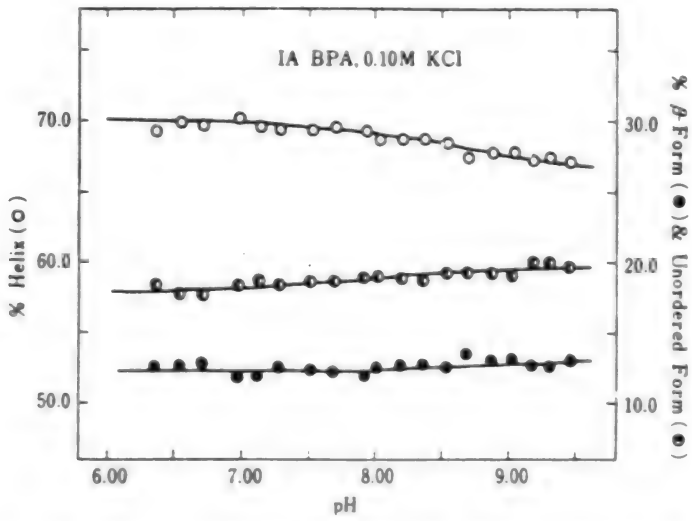

Fig. 8 Secondary structural change during the N→B transition (0.10 M KCl) of bovine plasma albumin (IA-BPA) in which SH groups are chemically modified with iodoacetamide[37]

We shall explain the opening and closing of the molecular crevices in the N→B transition. Kaplan, et al. used the previously described BPA, in which the SH groups of Cys-34 were labelled with nitroxide spin probes, and implied that the intramolecular crevices in the vicinity of Cys-34 open in two steps during the N→B transition as well, the same as in the case of the N→F transition, corresponding to alterations occurring as the rotary relaxation time of the spin probe in 0.10 M KCl decreases in two steps, i.e., the two-step decreases at pH 7.0~8.0 and pH 8.0~9.5.

As in the previous experiments for the N→F and F→E transitions, we examined the changes in the molecular rigidity in the N→B transition by f_2-irradiation of a specific side-chain proton and the use of the spin diffusion[15,30,37]. For

example, when 7.13 ppm (aromatic proton) is irradiated with appropriate power ($\gamma H_2/2\pi$, 69 Hz), the longer the cross-relaxation time (T_{1S}) to other side chains, the more flexible the molecule becomes. In Table 3, where salt concentration is noted as ~0 (~0 ionic strength), it means that alkali was added for pH adjustment, but no other salts were added. In such a state, the B-form has become more flexible compared to the N-form. However, as shown in Table 3, in the case of 0.10 M NaCl, f_2-irradiation of 7.13 ppm results in virtually no difference in the cross-relaxation time (T_{1S}) between the N- and B-forms. In other words, in the case of 0.10 M NaCl, no changes in molecular rigidity are observed with ^{1}H-NMR during the N→B transition. In order to examine what has become of the side-chain mobility, the N→B transition was examined using spin echo ^{1}H-NMR spectra as described in Fig. 5. There was virtually no difference in side-chain mobility between the N- and B-forms in the case of 0.10 M NaCl. When the ionic strength is ~0, the B-form side chain is mobile, and the result agrees with the change in cross-relaxation time (T_{1S}) shown in Table 3 (Fig. 17)[15,30,37].

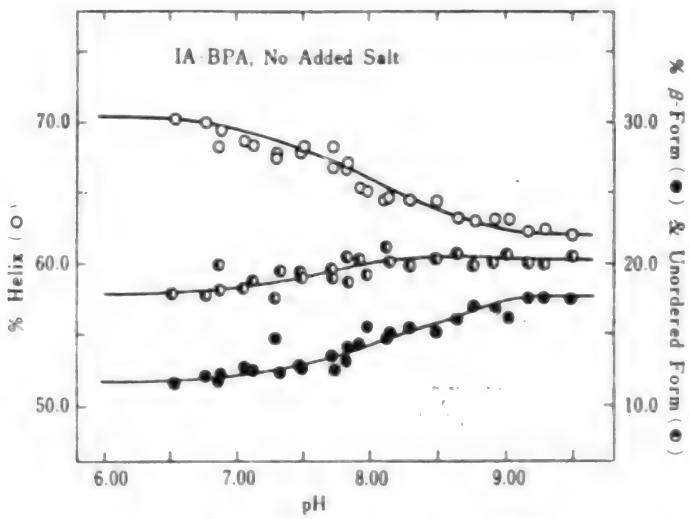

Fig. 9 Secondary structural change during the N→B transition (~0 ionic strength) of IA-BPA (see Fig. 8)[37]

Fig. 10 summarizes the major characteristics of the N→B transition. There are three domains in the plasma albumin molecule (Fig. 1). They are lined up like three suitcases [in the diagram]; and between the subdomains defined by dotted or solid lines (for example, subdomain 1AB, 1C) are hinges. In 0.10 M NaCl, the tertiary structure changes slightly when the N-form shifts to the B-form (Figs. 6 & 7), but almost no change occurs in the secondary structure. However, when various other experiments are conducted, for example, when the distance between Trp-214 and Tyr-411 (human serum albumin) was measured using Trp-fluorescent energy shifting, it is 18 Å in the N-form and increases in the B-form to 24 Å[4]. We determined the rotation relaxation time (Fig. 10, ρ(IA-BPA-$ANS_{0.9}$)) of an entire molecule, a complex (IA-BPA-$ANS_{0.9}$, IA-BPA/ANS=1/0.9) of BPA (IA-BPA) in which the SH groups were chemically modified with iodoacetamide and a fluorescent dye ANS (1-anilino-8-naphthalene-sulfonate). Although ANS is bound at the N-terminal of IA-BPA[40], the relaxation time was 131 nanoseconds in the

N-form and 113 nanoseconds in the B-form (see Fig. 10)[37]. Regarding the rotary relaxation time (ρ(DNS-HSA)) in the N→B transition pH region of human serum albumin (DNS-HSA) whose Lys was labelled with dansyl chloride, Preston, et al. reported[41] that ρ(DNS-HSA) decreases in the B-form. Dansyl chloride selectively reacts with the Lys of the CNBr-induced fragment C (124-298) (Fig. 1)[42]. Although each domain consists of two subdomains, when the N-form shifts to the B-form, we imagine that the rigidity of each subdomain probably does not change much. However, the movement between subdomains becomes more easily mediated by the hinges connecting the subdomains. If you imagine an actual model, I think two pieces of rod (corresponds to subdomains), which were initially tightly attached, become mobile in the B-form mediated by the chains like a chain-bound nunchaku (corresponds to domain) used in karate.

Table 3 ※ 3 Cross-Relaxation Times Obtained by the Inversion Recovery Method in Alkaline Region

pD(form)	Salt (M)	f_2(ppm)	$\gamma H_2/2\pi$(Hz)	T_{1s}(sec) $-CH_3$	ε-CH_2	Arom
6.27 (N)	~0	7.13	69	0.63	0.58	
9.14 (B)	~0	7.13	69	0.93	0.92	
6.27 (N)	~0	4.72	20	0.95	0.95	0.94
9.14 (B)	~0	4.72	20	1.21	1.24	1.10
6.27 (N)	~0	0.40	39	0.37	0.41	—
9.14 (B)	~0	0.40	39	0.57	0.60	0.48
6.27 (N)	~0	−2.45	107	1.02	1.04	1.28
9.14 (B)	~0	−2.45	107	1.49	1.96	1.28
6.96 (N)	0.10	7.13	69	0.73	0.64	
9.27 (B)	0.10	7.13	69	0.73	0.73	
6.96 (N)	0.10	0.40	39	0.52	0.65	0.58
9.27 (B)	0.10	0.40	39	0.64	0.63	0.82
6.96 (N)	0.10	4.72	20	1.41	1.30	1.37
9.27 (B)	0.10	4.72	20	1.33	1.35	1.22
6.96 (N)	0.10	−2.45	107	0.75	0.74	0.53
9.27 (B)	0.10	−2.45	107	0.78	0.68	0.87

N→B Transition (pI) 7.4-9.4)

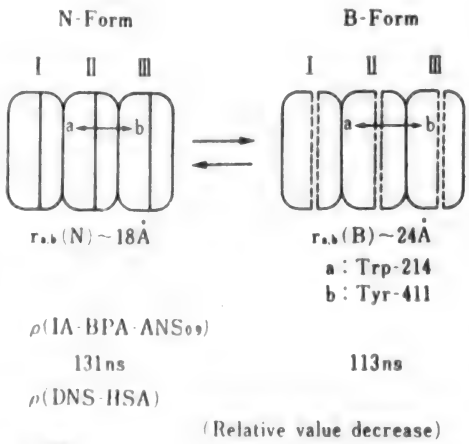

Fig. 10 Explanatory diagram of the N→B transition using 3-domain models; the areas demarcated with solid or dotted lines in each domain represent two subdomains connected by hinges. $r_{a,b}$(N) and $r_{a,b}$(B), respectively, show the distances between Trp-214 and Tyr-411 in the N- and B-forms[4]. ρ(IA-BPA-ANS$_{0.9}$): rotary relaxation time[37] of IA-BPA and the fluorescent dye, ANS complex; ρ(DNS-HSA): rotary relaxation time of dansylated human serum albumin. The subdomain-breathing state of the B-form is a state of each domain where the interaction between the subdomains connected with hinges weakens and the subdomains become readily mobile[37].

As explained in Fig. 10, we called the B-form the "subdomain-breathing state" for convenience. In general, when the B-form occurs following an N→B transition, the ability to bind metabolites and drugs increases. There are explanations (models) for this phenomenon. Brown, et al. postulated[1] that it is due to the increased mobility between subdomains mediated by hinges (Fig. 1). This corresponds to the Fig. 10 model. Furthermore, about 30 years ago, Karush postulated[42] that it is due to the fact that plasma albumin molecules have large "configurational adaptability," which we believe corresponds to the increased mobility between subdomains mediated by the hinges[1,37]. Wetlaufer and Lovrien reported that BPA's ability to bind and uncharged hydrophobic butane increased in the N→B transition (0.15 M KCl). Although the reduced viscosity of the BPA solution shows virtually no change in the N→B transition pH region, the phenomenon of increased ability to bind corresponds to Brown's model and Fig. 10. When an alkali-swollen form which occurs above pH 11 is reached, the reduced viscosity also increases and the ability to bind butane decreases sharply[44].

The phenomenon of turning a gel to sol by causing it to flow is called thixotropy; and the phenomenon of turning a sol to gel by causing it to flow is called rheopexy. It has been postulated that when hepatitis B virus invades the liver cells, polymerized human serum albumin (polyalbumin) and hepatitis B virus bind, and the resulting complex binds the albumin receptor on liver cells, which is then taken into the liver cells. However, not much polyalbumin is present in the bloodstream. When a flow of more than 5 cm per second is supplied, the BPA having a B-form structure becomes a large cluster which strongly scatters light, and when there is no velocity gradient, the cluster disappears. In other words, in the velocity gradient, there is a phenomenon of BPA or HSA clusters being formed by secondary binding, but they disperse when the flow ceases[45]. The physics group at the Nagoya University Faculty of Science discovered this phenomenon. The plasma albumin clusters reversibly formed in the above-mentioned velocity gradient may be involved in hepatitis B viral invasion of liver cells.

III. N-A isomerization reaction (intramolecular SH/S-S exchange reaction, molecular aging)[3,8]

Ordinarily, once the linear structure of a protein is determined, it is commonly believed that the 3-dimensional [3-D] structure can be determined on the same principle[46]. However, in the case of plasma albumin, the SH groups of Cys-34 and 17 S-S bonds are present, and the SH groups of Cys-34 act as catalysts for the intramolecular SH/S-S exchange reactions to carry out recombinations of the 17 S-S bonds[9-15]. In the example shown in Fig. 11, BMA is maintained at pH 8.6, 25°C and an ~0 ionic strength (no added salt). In Fig. 11, *N* denotes the non-aged form (here, *N*- and *A*-forms are shown in italics, the *N*-form contains both the *N*- and *B*-forms in the case of the N→B transition), and *A* denotes the aged form. After about 24 hours under the above-mentioned conditions, *N*/*A* approaches ~1/1. When this BMA solution is Tiselius-electrophoresed using pH 4.82, 0.03 M acetate buffer, two peaks corresponding to the *N*- and *A*-forms are observed as in Fig. 11 due to a large number of positive charges in the *A*-form (right side of Fig. 11). The analyses of the *N*- and *A*-forms are performed on the acidic side

because the SH/S-S exchange reactions virtually cease and the difference in the number of charges between *N*- and *A*-forms is the greatest. The left side of Fig. 11 also shows analytical results of cation-exchange high performance liquid chromatography (HPLC) using the differences in positive charges between the *N*- and *A*-forms. Starting at the top left side, the diagram shows HPLC profiles of the intramolecular aging reaction at 0 minute, 80 minutes, and 26 hours. The HPLC analyses also show *A/N* approaching ~1/1 as a result of an intramolecular aging reaction at 25°C, ~0 ionic strength, and pH 8.6. Although there are several kinds of *A*-form (aged form), when conditions are set to produce symmetric *N*-form peaks in the HPLC analysis, the *A*-form separates to the degree shown in Fig. 11[14,15]. Fig. 12 shows the increase in *A*-form at pH 8.6, 25°C, and ~0 ionic strength; i.e., analytical results of HPLC (•) of the periodic changes in $A/(N+A)$ and Tiselius electrophoresis (○)[14,15]. A very interesting point is that the *A*-form and *N*-form are in an almost 1:1 ratio. And, the *A*-form can revert (isomerization) to *N*-form[10,11,14,15]. We analyzed the *N-A* isomerization reaction using the following reversible linear reaction equation and not the third equation in Table 1.

$$N \underset{k_-}{\overset{k_+}{\rightleftarrows}} A$$

k_+ and k_- are, respectively, *N-A*, *A-N* reaction rate constants, and the apparent equilibrium constant, $K_{app}=k_+/k_-$. As shown in Fig. 12, k_+, k_-, and K_{app} obtained from HPLC are 5.7×10^{-5}/sec, 6.4×10^{-5}/sec, and 0.89, respectively. k_+, k_-, and K_{app} obtained from Tiselius electrophoresis are 4.1×10^{-5}/sec, 4.3×10^{-5}/sec, and 0.95, respectively. The apparent free energy change (ΔF) of *N-A* isomerization at pH 8.6, ~0 ionic strength, and 25°C is ~0 kcal/mol[10,13-15]. In other words, it infers the presence of more than two kinds of 3-D structures for the same free energy. In the case of BMA, these facts infer that the linear structure alone does not determine the 3-D structure.

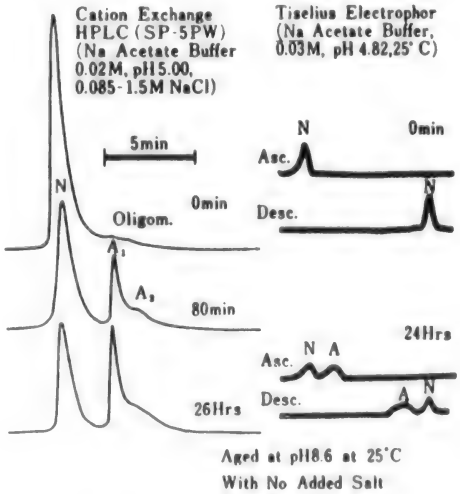

Fig. 11 Cation exchange HPLC profiles (left side) and Tiselius electrophoresis graph (right side) of bovine mercaptalbumin (BMA) which had undergone a molecular aging reaction (~0 ionic strength, pH 8.6, 25°C) In the diagram, *N* and *A* denote the non-aged form (*N*-form) and aged form (*A*-form), respectively[14,15].

The effects of ionic strength on k_+ and k_- are shown in Fig. 13[15]. They are shown by ○ and • for k_+ and △, ▲ for k_-. ○ and △ were obtained from the N⇌A reaction, a reaction from *N*-form to *A*-form; and • and ▲ show the reaction rate

constants obtained from an $A \rightleftarrows N$ reaction by adding salt to the reaction mixture solution of *N*- and *A*-form where *A/N* is ~1/1. When ionic strength is increased, k_+ decreases sharply, but k_- does not decrease as much, and the reaction progresses in the $A \rightarrow N$ direction.

Fig. 12 Time lapse of BMA (see Fig. 11) molecular aging (~0 ionic strength, pH 8.6, 25°C). •: $(A_1+A_2)/(N+A_1+A_2)$ obtained from HPLC; ○: $A/(N+A)$ obtained from Tiselius electrophoresis. k_1 [sic] and k_- are, respectively, $N \rightarrow A$, $A \rightarrow N$ reaction rate constants, K_{app} is k_+/k_-[14,15].

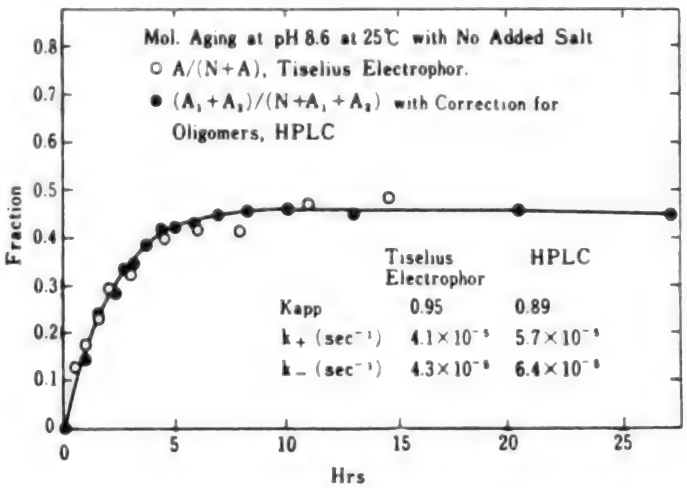

Fig. 13 Effects of ionic strength on k_+(○,•) and k_- (△,▲) during the *N-A* isomerization reaction[15]. See text for k_+ (•) and k_- (▲).

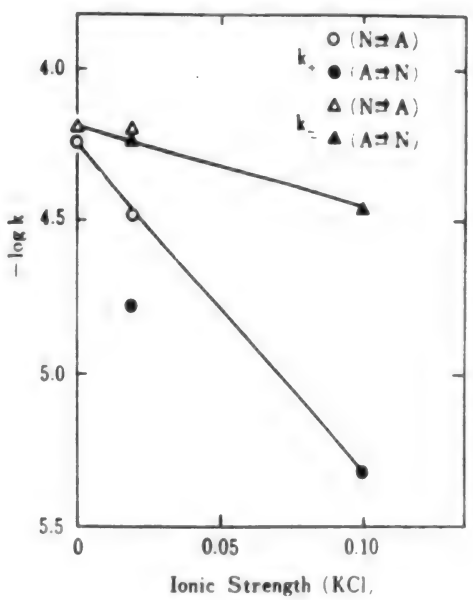

Fig. 14 shows the effects of temperature on k_+ and k_-. When the ionic strength is ~0, k_+ is indicated by ○, and k_-, by △. In the case of 0.10 M KCl, the BMA solution with an *A/N* ~1 is adjusted to 0.10 M⇄KCl as in Fig. 13, and k_+ (•) and k_- (▲) at 25°C, 30°C, and 35°C were obtained by using $A \rightleftarrows N$ reaction[15]. When the ionic strength is ~0, k_+/k_-~1 results and the apparent ΔF is almost 0 at any of the temperatures, 25°C, 30°C, or 35°C. In other words, *A/N* is ~1, and the Anfinsen theorem[46] stating that a linear structure determines 3-D structures on

the same principle does not apply in the case of a BMA solution with an ~0 ionic strength. Thermodynamic data, ΔF, ΔH, ΔS, ΔF', ΔH', and ΔS' in the cases of ionic strength of ~0 and 0.10 are shown at the bottom of Fig. 14[15].

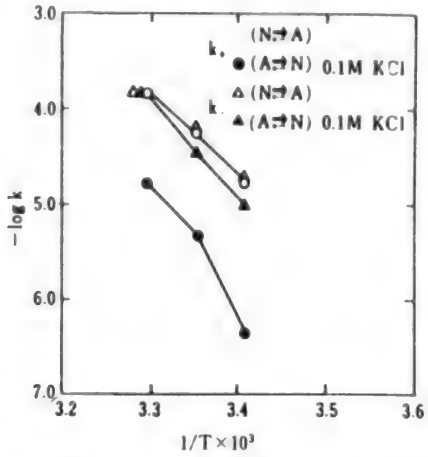

	ΔF (kcal/mol)	ΔH (kcal/mol)	ΔS (e.u.)	$\Delta F^{\ddagger}_{+}$ (kcal/mol)	$\Delta F^{\ddagger}_{-}$ (kcal/mol)	$H\Delta^{\ddagger}_{+}$ (kcal/mol)	$\Delta H^{\ddagger}_{-}$ (kcal/mol)	$\Delta S^{\ddagger}_{+}$ (e.u.)	$\Delta S^{\ddagger}_{-}$ (e.u.)
$\mu\sim0$	0.07	1.82	5.70	23.2	23.1	34.1	32.3	36.6	30.9
0.1 M KCl	1.20	15.3	47.3	24.7	23.5	63.0	47.7	128.5	81.2

Fig. 14 Effects of temperature on k_+(○,●) and k_-(△,▲) during the *N-A* isomerization reaction[15]. See text for k_+(●) and k_-(▲). Thermodynamic parameters are shown at the bottom.

The effect of pH on the *N-A* isomerization reaction are shown in Fig. 15[15]. In the vicinity of pH 7, the isomerization reaction rate is slow, and it is difficult to obtain k_+ (○) and k_- (△) using the *N⇄A* reaction. Consequently, isomerization was carried out at an ~0 ionic strength, pH 8.6, and 25°C to make *A/N* ~1; then the pH was adjusted to the measured pH, and k_+ (●), k_- (▲) obtained by using the *A⇄N* reaction is shown. This graph infers that the majority of the molecules are in the *N*-form structure in the pH range of 6.5~7.0. The method of measuring k_+ and k_- using the *A⇄N* reaction after adjusting the *A/N* to ~1 is a very useful method. For example, a fatty acid (sodium caprylate) used as a stabilizer for the heat treatment of human serum albumin for transfusion is added at an ~0 ionic strength to make caprylate/BMA =1~10 and the effect on k_+ and k_- were studied; virtually no effect was found on k_-, while k_+ sharply decreased at a molar ratio 5, and the reaction progresses *A→N*. It is interesting that the heat treatment stabilizer, which is used semiempirically, has an inhibitory action on the *N-A* isomerization reaction (molecular aging reaction) (it does not inhibit *A→N* reaction).

The α-helix content of the secondary structure of the *A*-form (aged form) has been reduced about 10 % compared to the *N*-form (non-aged form). In other words, the α-helix and ß-structure of the *A*-form in the vicinity of pH 7 are 60 % and 20 %, respectively, (~0 or 0.10 ionic strength). Even as the pH changed 7.0~9.0, no alteration was observed in the secondary structure of the *A*-form at

an ionic strength of either ~0 or 0.10. In the case of the *N*-form (non-aged form, IA-BPA), when the ionic strength is increased at, for example, pH 8.6~8.7, the α-helix content increases cooperatively at an ionic strength of 0.025→0.050 as shown in Fig. 16 (Fig. 15 [sic], ○). In the case of the *A*-form (aged form), the α-helix content does not increase. This mechanism infers that the aged form (*A* form) is a structure that appears to be "frozen" to the B-form structure of the non-aged form (*N*-form) at the ~0 ionic strength by means of an SH/S-S exchange reaction. Due to the fact that the *A*-form did not exhibit an N→F transition on the acidic side, it (the aged form) was previously considered to be a structurally frozen F-form (Table 1). However, we believe[47] that it is more like an S-S bond recombination structure frozen to the B-form (non-aged form) at an ~0 ionic strength. At an ~0 ionic strength and pH of 8.6~9.0, the B-form of the non-aged form (*N*-form) and the *A*-form (aged form) produced by the SH/S-S exchange reaction are believed to be structures in which the free energies are virtually equal (ΔF ~0).

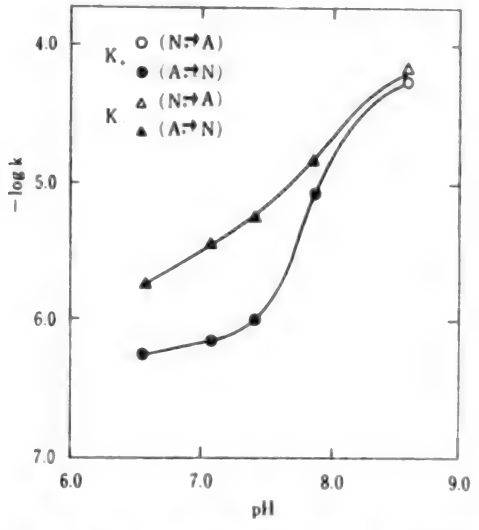

Fig. 15 pH effects of *N*-*A* isomerization reaction on k_+ (○,●), and k_- (△,▲)[15]. See text for k_+ (●) and k_- (▲)

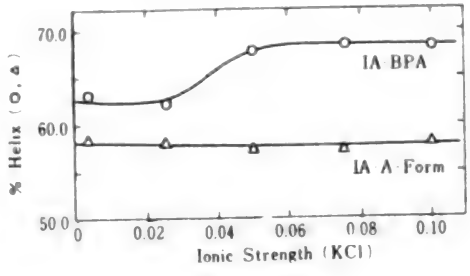

Fig. 16 Effect of ionic strength on the α-helix content of the non-aged form (*N*-form, IA-BPA, ○) and aged form (*A*-form, IA-*A*-form, △) whose SH groups are chemically modified with iodoacetamide at pH 8.6[47].

We measured the cross relaxation time, T_{1S} of the *A*-form at pD 7, 9 (0.10 M NaCl) and found it to be virtually the same as the non-aged form (*N*-form) (Table 3) in the same pD region. At an ionic strength of ~0, the T_{1S} value obtained by f_2 irradiation of 7.13 ppm ($\gamma H_2/2\pi$~69 Hz) is shown on the left side of Fig. 17. As in the case of the non-aged form, the T_{1S} value in the vicinity of pD9 shows a reduced molecular rigidity with respect to ^{1}H-NMR. Fig. 17 shows spin echo ^{1}H-NMR spectra for the non-aged form (*N*-form: pD 6.3, pD 9.1) and the aged form (*A*-form: pD 7.2, pD 9.4) at an ionic strength of ~0. In the case of the *A*-form, peaks of, for example, Lys ϵ-CH_2 (~3.0 ppm) and -CH_3 (~0.9 ppm) have become higher at both pD 7.2 and 9.4. As described above, these data suggest that, with respect to NMR, the side chain of the aged form is in a more mobile state compared with the non-aged form[15,47].

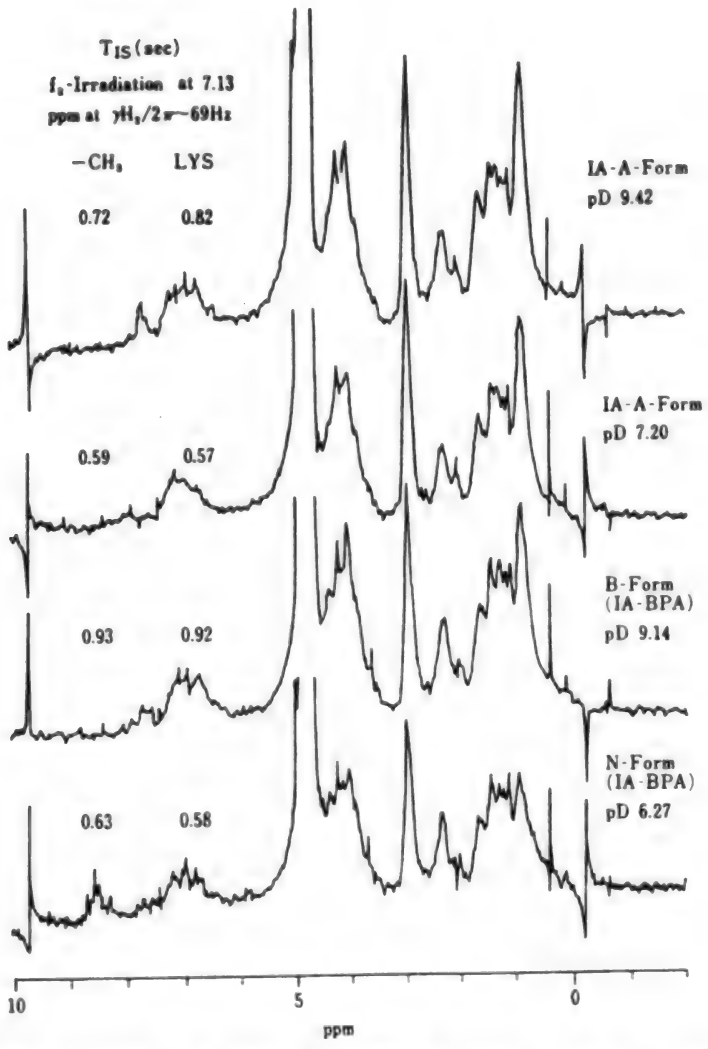

Fig. 17 Spin echo spectra (0.020 sec CPMG spectra) of non-aged form (*N*-form, IA-BPA) and aged form (*A*-form, IA-*A* form) at an ionic strength of ~0) (see Fig. 5). Shown on the left side is the cross relaxation time (T_{IS}) for f_2-irradiation at 7.13 ppm and $\gamma H_2/2\pi$~69 Hz[15,47]. 5.5% no added salt.

Table 4 is a summary of the molecular aging phenomena. The molecular aging phenomena are greatly influenced by temperature, ., and ionic strength during the intramolecular SH/S-S exchange reaction. Although we did not mention it in this section, the molecular volume of the aged form (*A*-form) was about 1.1 times greater than that of the non-aged form (*N*-form), the α-helix content decreased by about 10% (non-aged form (*N*-form), α-helix ~70%), and the side chains became mobile in the aged form (*A*-form) even in the neutral pD region (ionic strength ~0). However, the molecular rigidity of the aged form (*A*-form) estimated by the cross relaxation time (T_{IS}) was approximately the same as the non-aged form (*N*-form). The Tm and ΔHu obtained with differential scanning thermal analysis were 56.5°C and 116 kcal/mol, respectively, in the case of the aged form (*A*-form) and

62°C and 265 kcal/mol in the case of the non-aged form (*N*-form)[15,47]. As described, plasma (serum) albumin has very interesting characteristics in that "even when the linear structure is determined, the SH group of Cys-34 can become a catalyst depending on solvent conditions, and a different structure with recombined S-S bonds is produced." This phenomenon probably more closely resembles Klotz theory[48] which states that the autoplastic effect (linear structure) and alloplastic effect (solvent conditions, bonding ions, etc.) determine the 3-D structure rather than Anfinsen's theory[46] which states that the linear structure determines the 3-D structure[9,15].

Table 4

1. *N-A* isomerization (intramolecular SH, S-S exchange reaction) was affected by the following factors:
   Temperature
   pH
   Ionic strength
2. Vol(*A*)~1.1×Vol(*N*)
3. $f\alpha(A)\sim0.59$ (pH 7.0~9.0, $\mu=0.10$ or ~0)
   $f\alpha(N)\sim0.70$ (pH 7.0~9.0, $\mu=0.10$)
4. Motilities of side chains, segments etc.
   Side chains of the *A*-form: mobile
   ($T_{1S}(A)\sim T_{1S}(N)$)
5. DSC

	A	*N*
Tm (°C)	56.5	61.5
ΔHu (kcal/mol)	116	265

IV. Mercapt-non-mercapt conversion of human serum albumin and clinical reports[16-19,49,50]

Seventy-five percent of human serum albumin (HSA) is human mercaptalbumin (HMA) with an SH group on Cys-34. In addition, there are nonmercaptalbumin (human nonmercaptalbumin:HNA (CYS)), HNA (GSH) in which the SH group on Cys-34 changed to an S-S bond due, for example, to cysteine or glutathione attachment, as well as the nonmercaptalbumin (HNA (OXI)) in a further oxidized state, -SOH (sulfenic acid), $-SO_2H$ (sulfinic acid), and $-SO_3H$ (sulfonic acid)[19,50]. In the case of BPA, the presence of BNA (OXI) equivalent to HNA (OXI) has been reported by Janatova, et al. (1966), Fuller, et al. (1972), Wallevik (1976), and Takahashi, et al. (1983) (See reference 19). Regarding the presence of BNA (OXI), its biological significance has been pointed out related to problems of peroxide lipid.

The HMA and HNA in HSA can be easily separated and analyzed by HPLC using a special column[16-19]. Fig. 18 shows examples of separation and analysis of HMA and HNA using Asahipak GS-520 and the buffer solutions listed in the figure legend. KABI, CALBIO, NY, and KK are the abbreviated names of HSA manufacturers. The ratio of HMA (f_{HMA}) in the products are 0.65, 0.43, 0.52, and 0.47 as shown on the right side of Fig. 18. The values in parentheses were obtained by extending the tails of the HNA peaks slightly toward the right side in the image processing where f_{HMA} is obtained from HPLC profiles. For Fig. 18 HPLC, four Asahipak GS-520 columns were used, and the analysis time was 90 minutes. When 0.03M phosphate buffer and 0.30 M trisodium citrate (pH 6.80) are

used, HMA and HNA can be separated and analyzed with one GS-520 column in 30-40 minutes[19,50]. We have previously noted that HSA is composed of HMA, [HNA (CYS), HNA (GSH)], and HNA (OXI). When an Asahipak ES-502 N column is used, HMA, HNA (with S-S bonds), and HNA (OXI) can be separated. HNA's (with S-S bonds) include HNA (CYS) and HNA (GSH) (Fig. 19). In the HPLC profiles (Fig. 19), there are three peaks in the order of HMA, [HNA (CYS), HNA (GSH)], and HNA (OXI). When the buffer solutions listed in the legend for Fig. 19 legend are used with a 0→10% ethanol gradient, three components, HMA, [HNA (CYS), HNA (GSH)] and HNA (OXI) are separated[19,50]. The f_{HMA} values are shown on the right side of Fig. 19; they agree reasonably well with the f_{HMA} values in parentheses in Fig. 18.

Fig. 18

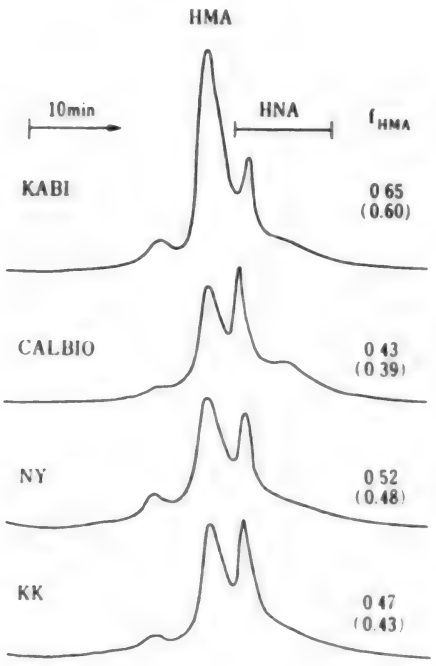

Fig. 19

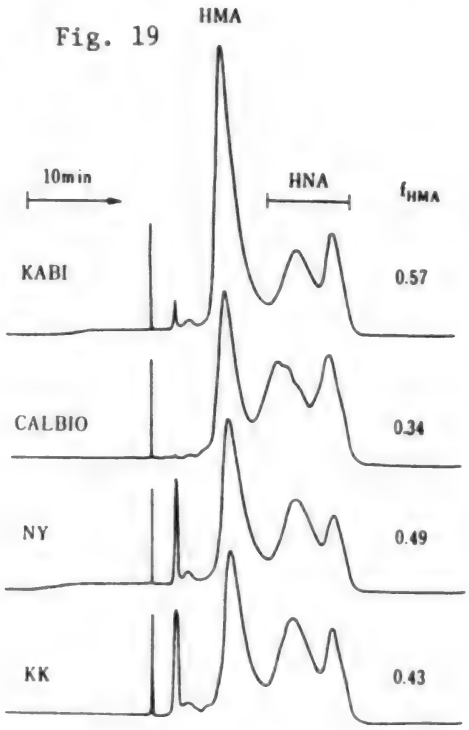

Fig. 18 HPLC profiles using Asahipak GS-520 (4 pcs) of human serum albumin (HSA) from various manufacturers[19,50]. HMA, HNA, and f_{HMA} denotes human mercaptalbumin, nonmercaptalbumin and HMA/(HMA+HNA). The f_{HMA} values in parentheses were obtained by slightly extending HNA to the right, which is the final eluent during the separation of the components. 0.03 M Na phosphate buffer, 0.15 M Na_2SO_4 (pH 6.87).

Fig. 19 HPLC profiles using Asahipak ES-502 N for HSA from various manufacturers[19,50]. 0.05 M Na acetate, 0.04 M Na_2SO_4 (pH 4.80). Ethanol concentration gradient 0→10%

Sera from elderly subjects who have no hepatic or renal impairments were provided by the Municipal Medical Center for the Aged, and HSA changes in the reduced form albumin (HMA) content were analyzed[19]. Changes in the HMA and HNA of elderly's HSA were studied comparatively with three kinds of HPLC. In other words, we used Asahipak GS-520 (4 pcs) (eluent, Fig. 18 bottom), GS-520 (1 pc)

(eluent, 0.03 M phosphate buffer, 0.30 M trisodium citrate (pH 6.89)), and ES-520 N (1 pc) (eluent, Fig. 19 bottom). The mean of f_{HMA} values, f_{HMA}±SD, obtained by HPLC were 0.48±0.05 (n=114), 0.47±0.06 (n=114), and 0.43±0.06 (n=55), respectively. The $\bar{f}_{HMA}$ of healthy adult men was 0.75±0.028 (n=28), and there was a significant difference between the two groups (p<0.001). In the case of healthy elderly subjects, HNA, i.e., the oxidized form of HSA increases, and its reduced form decreases. It has been reported (1983)[51] that the number of SH groups of crystalline proteins decreases with age. The decrease in the reduced form (HMA) of HSA shows exactly the same trend as the decrease in SH groups of crystalline proteins[19]. Having received additional supply from the Municipal Medical Center for the Aged, we analyzed these sera of elderly people with HPLC using GS-520 (1 pc). When we summarized the result along with the previously mentioned data, $\bar{f}_{HMA}$ (60~99) is 0.48±0.059 (n=183) (Numerical ranges in parentheses denote age). The $\bar{f}_{HMA}$ (60~69), $\bar{f}_{HMA}$ (70~79), $\bar{f}_{HMA}$ (80~89), and $\bar{f}_{HMA}$ (90~99) were 0.52±0.044 (n=47), 0.48±0.053 (n=43), 0.46±0.054 (n=81), and 0.47±0.076 (n=12), respectively.

We analyzed the characteristic changes (f_{HMA}) of HSA in renal diseases, especially in chronic renal insufficiency. The $\bar{f}_{HMA}$ in healthy adults is 0.75±0.028 (n=28), whereas the $\bar{f}_{HMA}$ of chronic renal insufficiency (non-hemodialysis) patients is 0.51±0.096 (n=28), and there is a significant difference between the two groups (P<0.001)[49,52]. In other words, the sera from such renal insufficiency patients tended to contain more of the oxidized form. In addition, there is a significant negative correlation between $\bar{f}_{HMA}$ and serum creatinine level of chronic renal insufficiency patients (r=-0.85, P<0.05). When chronic renal insufficiency patients undergo artificial dialysis, one can observe the changes shown in Fig. 20. Fig. 20 shows one example of dialysis results; the HNA is very high before dialysis, it decreases after 5-hour dialysis and the HMA increases (HNA→HMA conversion). The fact that HNA is high at the inlet of dialyzer and HNA has decreased at the outlet is a very interesting phenomenon. When we compare the HPLC profile of HSA at time 0 min. and 300 min of dialysis, we see a very symmetric change in the pattern. A summary of various mean values for hemodialysis (HD) patients (Sawada Hospital, Gifu) is as follows[17,18] (Virtually the same results were obtained with hemodialysis patients at Hayatoku Hospital in Gifu):

$\bar{f}_{HMA}$ (before HD) =0.40±0.09 (n=122)
Mean of [f_{HMA} (after HD) - f_{HMA} (before HD)]
=0.17±0.08 (n=110, P<0.001)
Mean of [f_{HMA} (outlet) - f_{HMA} (inlet)]
=0.09±0.05 (n=122, P<0.001)

Following hemodialysis, as the oxidized forms of sulfur-containing amino acids such as cystine increase in the bloodstream, cystine reacts with HMA resulting in HMA + cystine ⇄ HNA + cysteine. The cysteine is readily oxidized in the bloodstream to become cystine, and this cystine reacts with HMA and produces HNA. Through these reactions, a considerable fraction of the predialysis HSA changes to HNA. Although the mechanism is unknown, the HNA→HMA change is due to hemodialysis as shown in Fig. 20. In other words, HSA in dialysis patients undergoes repetitious HNA⇄HMA conversions in the bloodstream.

Fig. 20 HNA→HMA conversion due to hemodialysis (chronic renal insufficiency)[19,50]. The HPLC profiles at predialysis (0 min.), dialyzer inlet and outlet after 30 min, and postdialysis (300 min, dialyzer inlet) are shown. See Fig. 18 for column and eluent.

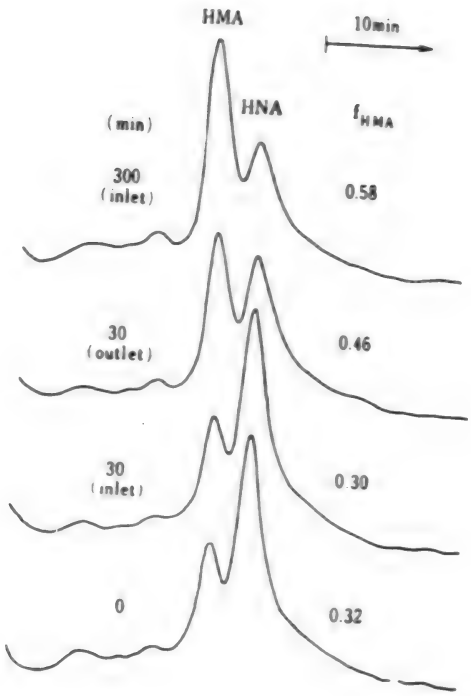

To what extent the HSA of hemodialysis patients with chronic renal insufficiency as shown in Fig. 20 undergo HNA→HMA conversion following kidney transplant and how closely it approaches f_{HMA} of healthy subjects are very interesting issues. Table 5 shows the analytical results of f_{HMA} values of many kidney transplant patients' sera provided by the Kidney Center at the Kitasato University Medical School in a collaborative study[52]. There were significant differences in the f_{HMA} values of HSA from transplant patients in hospitals A and B who had not used cyclosporin A ($P<0.001$). In addition, there was a very large difference in f_{HMA} values among the groups using cyclosporin A as shown in Table 5 ($P<0.001$). The reason for the difference between hospitals A and B is unknown.

We have explained HSA's structural changes (HMA⇄HNA conversion) in chronic renal insufficiency, chronic renal insufficiency hemodialysis, and kidney transplants. In addition to these diseases, we have analyzed HSA, i.e., f_{HMA} values in chronic articular rheumatism, various liver diseases, and various endocrine and metabolic diseases. For reference, we shall explain changes in f_{HMA} values caused by liver diseases or the use of glucocorticoids. As shown in Table 6, significant changes occurred in f_{HMA} values in cases of chronic hepatitis (CH), liver cirrhosis (compensated) (LC(c)), liver cirrhosis (decompensated) (LC(d)), hepatocellular carcinoma (HCC), acute hepatitis (AH), and fulminant hepatic failure (FHF). Incidentally, Table 6 includes data only of patients with no renal disorders (collaborative study with the First Internal Medicine Department, University of Gifu School of Medicine)[18]. The HSA of nephrotic syndrome patients hospitalized in the above University Hospital also showed a very high HNA compared to that of healthy adults. One factor contributing to increased HNA may be the use of glucocorticoids discussed later or the use of albumin with very high HNA for transfusion[53]. A marked decrease in HMA was

observed in an untreated patient with Addison's disease (48-year-old, ♀) (f_{HMA}=0.47, Fig. 21 (1)). As shown at the bottom of Fig. 21, when we administered various glucocorticoids to this patient, the f_{HMA} values changed from 0.43 → 0.35 → mostly HNA → 0.72 → 0.71 →.....(Fig. 21 (2) → (3) → (4) → (5) → (6) →.....) and have approached the 0.75 value of a healthy adult by continued use of the glucocorticoids[53]. There are reports[54-56] that a one-time large dose administration of glucocorticoid to animals increased peroxides in the bloodstream, decreased glutathione, and increased glutathione after 7-10 days. As in Fig. 21, the phenomenon of decreased HMA (reduced form), i.e., increased HNA (oxidized form), followed by increased HMA is a series of changes that is similar to those observed in animal experiments (collaborative study with the Third Internal Medicine Department, University of Gifu School of Medicine).

Table 5 表 5 $\bar{f}_{HMA}$ Values in Renal Transplants with or without Cyclosporin A (Cy-A)

			Control	Renal Transplant	
				(A-Hospital)	(B-Hospital)
	Cy-A(−)	$\bar{f}_{HMA}\pm SD$	0.75±0.028	0.63±0.083	0.55±0.080
		n	28	116	68
1984					
∫					
1986					
	Cy-A(+)	$\bar{f}_{HMA}\pm SD$	—	0.63±0.064	0.49±0.089
		n	—	26	33
1988		$\bar{f}_{HMA}\pm SD$	—	0.59±0.063	
		n		78	

**: $P<0.01$, ***: $P<0.001$

Acknowledgement

Finally, we would like to thank Professors K. Miura, Y. Muto (Gifu University School of Medicine), K. Koshiba (Kitasato University School of Medicine), T. Oka (Kyoto Prefectural University of Medicine), Drs. S. Sawada (Sawada Hospital, Gifu) and I. Hayano (Hayatoku Hospital, Gifu) for their generous cooperation in the studies of HMA≠HNA conversion. The ^{1}H-NMR data shown is part of the results from collaborative studies with the physiology research laboratory (Prof. H. Watari, 1981-1989). Our sincere gratitude is also expressed to our colleagues in the department, Dr. K. Kuwata and N. Uno.

(Footnote)

Carter, et al.[57] published (1989) a 6.0Å-resolution X-ray diffraction pattern of human serum albumin (HSA) crystallized from polyethylene glycol (pH 6.8-7.2). HSA is a protein with a large number of α-helices. Brown, et al.[1,2] described hinges (see Fig. 1) connecting subdomains, i.e., 102-123, 290-315, and 488-513

to form a fair number of helical segments, and 178-199, 370-391 that connect domains that are nonhelical segments. These results are very similar to the secondary structure of HSA estimated by McLachlan, et al.[58] from the linear structure. Carter, et al.[57], unlike Brown, et al.[1,2], labelled subdomains as IA, IB, IIA, IIB, IIIA, and IIIB. As shown in Fig. 22, [IA, IB, IIA] and [IIB, IIIA, IIIB] form separate clusters.

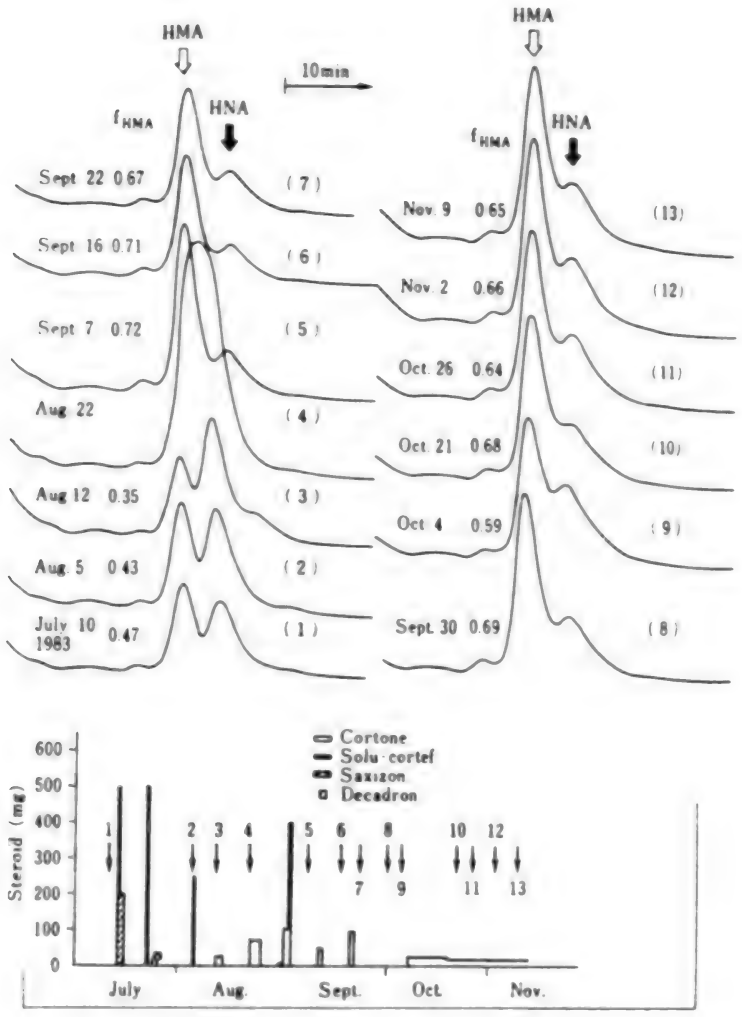

Fig. 21 HPLC profiles of HSA from an Addison's disease patient (48-year-old, ♀). An Asahipak GS-520 (4 pcs) was used with 0.10 M phosphate buffer and 0.30 M NaCl (pH 6.86). The diagram at the bottom shows glucocorticoid administration status. Before treatment (1) with glucocorticoid, and after therapy began (2-13)[49,53].

Table 6 表 6 T_{max} Values in Patients with Various Liver Diseases*

Parameter	Control	CH	LC(c)	LC(d)	LC(c) and HCC	AH	FHF
T_{max}	0.75±0.028	0.64±0.053	0.64±0.050	0.49±0.076	0.52±0.073	0.64±0.046	0.33
n	28	23	9	9	10	5	2

***
***
***
***
***
***
***
***
**
***

* CH = chronic hepatitis ; LC(c) = liver cirrhosis (compensated) ; LC(d) = liver cirrhosis (decompensated) ; HCC = hepatocellular carcinoma ; AH = acute hepatitis ; FHF = fulminant hepatic failure.
** $P < 0.01$. *** $P < 0.001$.

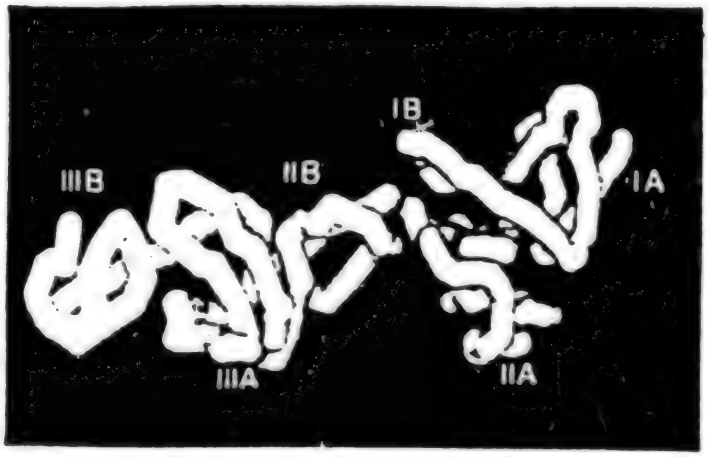

Fig. 22 X-ray diffraction pattern of Human Serum Albumin (HSA)

References:

1. Brown, J. R. & Shockley, P.: Serum albumin: Structure and characterization of its ligand binding sites. In: Lipid-Protein Interaction. Vol 1. Jost, P. C. & Griffith, O. H. eds. New York, John Wiley & Sons (1982) pp. 26-28

2. Brown, J. R.: Serum albumin: Amino acid sequence. In: Albumin Structure, Function and Uses. Rosenoer, V. R., Oratz, M. & Rothschild, M. A. eds. Oxford, Pergamon Press (1977) pp. 27-51

3. Era, S., Kuwata, K., Nagaoka, T., Sogami, M., Kato, K., Watari, H., & Akasaka, K.: Study of bovine plasma albumin structural transition by cross relaxation time and spin echo spectra, Proceedings of the 27th NMR Forum, pp. 87-90 (1988)

4. Hagag, N. G., Birnbaum, E. R. & Darnall, D. W.: Distance between Tyr-411 and Trp-214 of human serum albumin measured by fluorescence energy transfer: Effects of pH and fatty acid, Federation Proc. 41: 1189(1982)

5. Brown, J. R., Tavasolian, B., Shockley, P., Tallon, K., Barr, E. & Brown, K.: Serum albumin: Structure and characterization of its binding sites, 14th Internat. Congr. Biochem. Abstracts 3: 16(1988)

6. Era, S., Ashida, H., Nagaoka, S., Inouye, H. & Sogami, M.: CD-resolved secondary structure of bovine plasma albumin in acid-induced isomerization, Int. J. Peptide Protein Res. 22: 333(1983)

7. Era, S., Nagaoka, S., Sogami, M., Watari, H. & Akasaka, K.: Sodium dodecyl sulfate-bovine plasma albumin complex: Structural transition from native to relatively compact globule forms with mobile side chains in acidic region--N-F transition, Int. J. Peptide Protein Res. 26: 21(1985)

8. Foster, J. F.: Some aspects of the structure and conformational properties of serum albumin. In: Albumin Structure, Function and Uses. Rosenoer, V. R., Oratz, M. & Rothschild, M. A. eds. Oxford, Pergamon Press (1977) pp. 53-84.

9. Sogami, M., Peterson, H. A. & Foster, J. F.: The microheterogeneity of plasma albumin. V. Permutations in disulfide pairing as a probable source of microheterogeneity in bovine albumin, Biochemistry 8: 49(1969)

10. Nikkei, H. J. & Foster, J. F.: A reversible sulfhydryl-catalyzed structural alteration of bovine mercaptalbumin, Biochemistry 10: 4479(1971)

11. Stroupe, S. D. & Foster, J. F.: Further studies of the sulfhydryl-catalyzed isomerization of bovine mercaptalbumin, Biochemistry 12: 3824(1973)

12. Wallevik, K.: S-S-interchanged and oxidized isomers of bovine serum albumin separated by isoelectric focusing, Biochem. Biophys. Acta 420: 42(1976)

13. Inouye, H., Era, S., Sakata, S., Kuwata, K. & Sogami, M.: Intra-molecular sulfhydryl-catalyzed structural alteration of bovine serum albumin: N-A isomerization, Int. J. Peptide Protein Res. 24: 337(1984)

14. Kuwata, K., Era, S., Inouye, H. & Sogami, M.: Ion-exchange high-performance liquid chromatographic studies on sulfhydryl-catalyzed structural alterations of bovine mercaptalbumin, J. Chromatogr. 332: 29(1985)

15. Kuwata, K., Era, S., Sogami. M. & Watari, H.: Molecular aging and aged structure of bovine mercaptalbumin, Gifu University Medical Bulletin 36: 479(1988)

16. Sogami, M., Nagaoka, S., Era, S., Honda M & Noguchi, K.: Resolution of human mercapt- and nonmercaptalbumin by high-performance liquid chromatography, Int. J. Peptide Protein Res. 24: 96(1984)

17. Sogami, M., Era, S., Nagaoka, S., Kuwata, K., Kida, K., Miura, K., Inouye, H., Suzuki, E., Hayano, S. & Sawada, S.: HPLC-studies on nonmercapt-mercapt conversion of human serum albumin, Int. J. Peptide Protein Res. 25: 398(1985)

18. Sogami, M., Era, S., Nagaoka, S., Kuwata, K., Kida, K., Shigemi, J., Miura, K., Suzuki, E., Muto, Y., Tomita, E., Hayano, S., Sawada, S., Noguchi, K. & Miyata, S.: High-performance liquid chromatographic studies on nonmercapt ⇄ mercapt conversion of human serum albumin

19. Era, S., Hamaguchi, T., Sogami, M., Kuwata, M. K., Suzuki, E., Miura, K., Kawai, K., Kitazawa, Y., Okabe, H., Noma, A. & Miyata, S.: Further studies on the resolution of human mercapt- and nonmercaptalbumin and on human serum albumin in the elderly by high-performance liquid chromatography, Int. J. Peptide Protein Res. 31: 435(1988)

20. Hagenmaier, R. D. & Foster, J. F.: Preparation of bovine mercaptalbumin and an investigation of its homogeneity, Biochemistry 10: 637(1971)

21. Tanford, C., Buzzell, J., Rands D. & Swanson, S.: The reversible expansion of bovine serum albumin in acid solutions, J. Am. Chem. Soc. 77: 6421(1955)

22. Sogami, M. & Ogura, S.: Structural transition of bovine plasma albumin--Location of tyrosyl and tryptophyl residues by solvent pertubation difference spectra, J. Biochem. 73: 323(1973)

23. Hull, H. H. Chang, R. & Kaplan, L. J.: On the location of the sulfhydryl group in bovine plasma albumin, Biochem. Biophys. Acta 400: 132(1975)

24. Cornell, C. N. & Kaplan, L. J.: Spin-label studies of the sulfhydryl environment in bovine plasma albumin. 1. The N-F transition and acid-expansion, Biochemistry 17: 1750(1978)

25. Cornell, C. N. & Kaplan, L. J.: Spin-label studies of the sulfhydryl environment in bovine plasma albumin. 2. The neutral transition and the A isomer, Biochemistry 17: 1755(1978)

26. Wishnia, A. & Pinder, T.: Hydrophobic interactions in proteins: Conformational changes in bovine serum albumin below pH 5, Biochemistry 3: 1377(1964)

27. McMenamy, R. H.: The binding of indole analogues to defatted human serum albumin at different chloride concentration, J. Biol. Chem. 239: 28(1964)

28. Akasaka, K.: Longitudinal relaxation of protons under cross saturation and spin-diffusion, J. Magn. Resonance 45: 337(1981)

29. Akasaka, K.: Spin-diffusion and the dynamic structure of a protein. Streptomyces subtilisin inhibitor, J. Magn. Resonance 51: 14(1983)

30. Era, S., Kuwata, K., Nagaoka, T., Sogami, M., Kato, K., Watari, H., & Akasaka, K.: Study of bovine plasma albumin structural transition by cross relaxation time and spin echo spectra, Proceedings of the 27th NMR Forum, pp 87-90 (1988)

31. Vijai, K. K. & Foster, J. F.: The amphoteric behavior of bovine plasma albumin. Evidence for masked carboxylate groups in the native protein, Biochemistry 6: 1152(1967)

32. Leonard, W. J. Jr., Vijai, K. K. & Foster, J. F.: A structural transformation in bovine and human plasma albumins in alkaline solution as revealed by rotatory dispersion studies, J. Biol. Chem. 238: 1984(1963)

33. Harmsen, B. J. M., DeBruin, S. H., Janssen, L. H. M., DeMiranda, J. F. R. & Van Os, G. A. J.: pK change of imidazole groups in bovine serum albumin due to the conformational change at neural pH, Biochemistry 10: 3217(1971)

34. Zurawski, V. R. Jr. & Foster, J. F.: The neutral transition and the environment of the sulfhydryl side chain of bovine plasma albumin, Biochemistry 13: 3465(1974)

35. Leonard, W. J. Jr. & Foster, J. F.: Changes in optical rotation in the acid transformations of plasma albumin. Evidence for the contribution of tertiary structure to rotatory behavior, J. Biol. Chem. 236: 2662(1961)

36. Sogami, M. & Foster, J. F.: Isomerization reaction of charcoal-defatted bovine plasma albumin. The N-F transition and acid expansion, Biochemistry 7: 2172(1968)

37. Era, S., Itoh, K. B., Sogami, M., Kuwata, K., Iwama, T., Yamada, H. & Watari, H.: Structural transition of bovine plasma albumin--the N-B transition, Int. J. Peptide Protein Res. (in press, 1989)

38. Fuller Noel, J. K. & Hunter, M. J.: Bovine mercaptalbumin and nonmercaptalbumin. Interconversions and structural differences, J. Biol. Chem. 247: 7391(1972)

39. Hilak, M. C., Harmsen, B. J. M., Braam, W. G. M., Joordens, J. J. M. & Van Os, G. A. J.: Conformational studies on large fragments of bovine serum albumin in relation to the structure of the molecule, Int. J. Peptide Protein Res. 6: 95(1974)

40. Era, S., Kuwata, K., Kida, K., Sogami, M. & Yoshida, A.: Circular dichroic and fluorometric studies on the acid-induced, isomerization of bovine plasma albumin-1-anilino-8-naphthalenesulfonate complex, Int. J. Peptide Protein Res. 26: 575(1985)

41. Preston, B. N., Obrink, B. & Laurent, T. C.: The rotational diffusion of albumin in solutions of connective-tissue polysaccharides, Eur. J. Biochem. 33: 401(1973)

42. McMenamy, R. H.: Albumin binding sites. In: Albumin Structure, Function and Uses. Rosenoer, V. R., Oratz, M. & Rothschild, M. A. eds. Oxford, Pergamon Press (1977) pp. 143-158

43. Karush, F.: Heterogeneity of binding sites of bovine serum albumin, J. Am. Chem. Soc. 72: 2705(1959)

44. Wetlaufer, D. B. & Lovrein, R.: Induction of reversible structural changes in proteins by nonpolar substances, J. Biol. Chem. 239: 596(1964)

45. Hirakawa, H., Yoshino, S., Imai, N. & Sogami, M.: Cluster formation of a charged polymer in a velocity gradient field, Seibutsu Butsuri [Biophysics] 29: 392(1989)

46. Anfinsen, C. B.: The tertiary structure of ribonuclease, Brookhaven Symp. Biol. 15: 184(1962)

47. Era, S., Kuwata, K., Sogami, M. & Watari, H.: Circular dichroic and ^{1}H-n.m.r. studies on the aged form of bovine mercaptalbumin, Int. J. Peptide Protein Res.(Paper to be presented)

48. Klotz, I. M.: Protein conformation: autoplastic and alloplastic effects, Arch. Biochem. Biophys. 116: 92(1966)

49. Sogami, M. & Era, S.: Serum albumin and disease, Taisha [Metabolism] 22: 1217(1985)

50. Sogami, M. & Era, S. & Kuwata, K.: Protein abnormality - Structural changes in human serum albumin in chronic renal insufficiency, Jin to Toseki [Kidney and Dialysis] 23: 651(1987)

51. Kuck, J. F. R., Yu, N. T. & Askren, C. C.: Total sulfhydryl by Raman spectroscopy in the intact lens of several species: Variations in the nucleus and along the optical axis during aging, Exp. Eye Res. 34: 23(1982)

52. Era, S., Kuwata, K., Sogami, M., Suzuki, E., Kumano, K., Sakai, T. Koshiba, K., Yanagihara, Y. & Noguchi, K.: High-performance liquid chromatographic study of serum albumin structural changes (nonmercapt→mercapt conversion) in kidney transplant patients, LST Society Journal 2: 203(1988)

53. Suzuki, E., Takeda, N., Sakada, S., Yasuda, K., Era, S., Kuwata, K., Sogami, M. & Miura, K.: Oxidation-reduction reactions of serum albumin in endocrine and metabolic diseases, Gifu University Medical Bulletin 36: 500(1988)

54. Nishigori, H., Lee, J. W., Iwamoto, Y., Hayashi, R., Maruyama, K. & Iwatsuru, M.: Alteration of hepatic lipid peroxide levels during cataract formation caused by glucocorticoids in developing chick embryos, Life Sci. 35: 981(1984)

55. Nishigori, H., Hayashi, R., Lee, J. W. & Iwatsuru, M.: Effect of MPG on glucocorticoid-induced cataract formation in developing chick embryos, Invest. Ophthalmol. Vis. Sci 25: 1051(1984)

56. Nishigori, H., Lee, J. W., Yamauchi, Y. & Iwatsuru, M.: Elevation of blood lipid peroxide (TBA-reacting substance) level in developing chick embryos after glucocorticoid administration, Biochem. Internat. 13: 147(1986)

57. Carter, D. C., He, X., Munson, S. H., Twigg, P. D., Gernert, K. M., Broom, M. B. & Miller, T. Y.: Three-dimensional structure of human serum albumin, Science 244: 1195(1989)

58. McLachlan, A. D. & Walker, J. E.: Serum albumin domain secondary structure prediction, Biochem. Biophys. Acta 536: 106(178)

- END -

END OF FICHE

DATE FILMED

5 April 1991